



ELSEVIER

Contents lists available at SciVerse ScienceDirect

Journal of Magnetism and Magnetic Materials

journal homepage: www.elsevier.com/locate/jmmm

Low-field large reversible magnetocaloric effect in the RNi_2Si_2 ($R=Dy, Ho, Er$) compounds

Wenliang Zuo*, Fengxia Hu, Sun Jirong, Baogen Shen*

State Key Laboratory for Magnetism, Institute of Physics, Chinese Academy of Sciences, Beijing 100190, People's Republic of China



ARTICLE INFO

Article history:

Received 11 January 2013

Received in revised form

19 March 2013

Available online 4 June 2013

Keywords:

 RNi_2Si_2 compound

Magnetocaloric effect

Magnetic entropy change

ABSTRACT

The magnetocaloric effect (MCE) of RNi_2Si_2 ($R=Dy, Ho, Er$) compounds with the $ThCr_2Si_2$ -type body-centered tetragonal structure are investigated. RNi_2Si_2 compounds are antiferromagnetic (AFM) with Néel temperature $T_N=6.5$ K, 4.9 K, and 3.5 K, respectively. A field-induced metamagnetic transition from AFM-to-ferromagnetic (FM) state is found below T_N , which leads to a large MCE around the T_N . The maximal values of magnetic entropy change (ΔS_M) for RNi_2Si_2 ($R=Dy, Ho, Er$) reach -6.9 , -10.9 , and -15.1 $Jkg^{-1}K^{-1}$ and -21.3 , -21.7 , and -21.3 $Jkg^{-1}K^{-1}$ without thermal and magnetic hysteresis losses for the field changes of 0–2 T and 0–5 T, respectively. The large ΔS_M is associated with the field-induced first-order AFM–FM metamagnetic transition and low critical field. The excellent MCE under low field change without hysteresis loss suggests that RNi_2Si_2 ($R=Dy, Ho, Er$) can be an appropriate candidate for magnetic refrigerant in liquid helium temperature ranges.

© 2013 Elsevier B.V. All rights reserved.

1. Introduction

Recently, magnetic refrigeration based on the magnetocaloric effect (MCE) of a magnetic material has attracted much attention due to its higher energy efficiency and friendly environment compared to conventional gas compression refrigeration [1–5]. The MCE is related to the isothermal magnetic entropy change (ΔS_M) or the adiabatic temperature change (ΔT_{ad}) of a material when exposed to a varying magnetic field. The large values of ΔS_M and ΔT_{ad} are considered to be the most important requirements. In addition, the negligible thermal and magnetic hysteresis losses are also necessary for practical application.

During the last few years, some RT_2X_2 (R =rare earth, T =transition metal, and $X=Si, Ge, B$, etc.) compounds have been found to possess not only large MCE but also a small hysteresis loss around their ordering temperature [6–13]. The observed giant MCE is mainly associated with a field-induced first-order metamagnetic transition from antiferromagnetic (AFM) to ferromagnetic (FM) states [6,8,10–13], and a small number of second-order phase transitions [7,9,13]. Most RNi_2Si_2 compounds crystallize in a $ThCr_2Si_2$ -type body centered tetragonal structure and have AFM structure at low temperatures [14,15]. Furthermore, the phase transition temperature is very low. Therefore, the RNi_2Si_2 compounds possibly are potential magnetic refrigerants for the gas liquefiers. In this paper, the MCE of RNi_2Si_2 ($R=Dy, Ho, Er$) compounds were systematically studied. Low field large MCE around its own ordering temperature with negligible

thermal and magnetic hysteresis losses are observed. The result suggested that RNi_2Si_2 ($R=Dy, Ho, Er$) compounds are probably promising candidates for magnetic refrigerants working at low temperatures (particularly in the liquid helium region).

2. Experiment

The RNi_2Si_2 ($R=Dy, Ho, Er$) compounds were prepared by arc-melting in a high purity argon atmosphere. The purities of starting materials were higher than 99.9%. The ingots were melted five times to ensure homogeneity and then annealed at 1073 K for 7 days under vacuum and rapidly quenched to room temperature. The phase structure and crystal lattice parameters were examined at room temperature by X-ray powder diffraction with $Cu K\alpha$ radiation. Magnetizations were measured as functions of temperature and magnetic field by using a commercial superconducting quantum interference device (SQUID) magnetometer, Model MPMS-7 from Quantum Design Inc. The temperature dependent magnetizations were measured in both zero field-cooled (ZFC) and field-cooled (FC) processes. With the sample cooled down to 2 K in a zero field, the heating curve from 2 to 50 K was measured in a magnetic field of 0.01 T and the cooling curve from 50 to 2 K was measured also in the same field.

3. Result and discussion

Fig. 1 shows the measured and refined powder X-ray diffraction (XRD) patterns of RNi_2Si_2 ($R=Dy, Ho, Er$) compounds at room

* Corresponding authors. Tel.: +86 01082649251, +86 01082648082.

E-mail addresses: wzuo@iphy.ac.cn (W.-n. Zuo), shenbg@aphy.iphy.ac.cn (B. Shen).

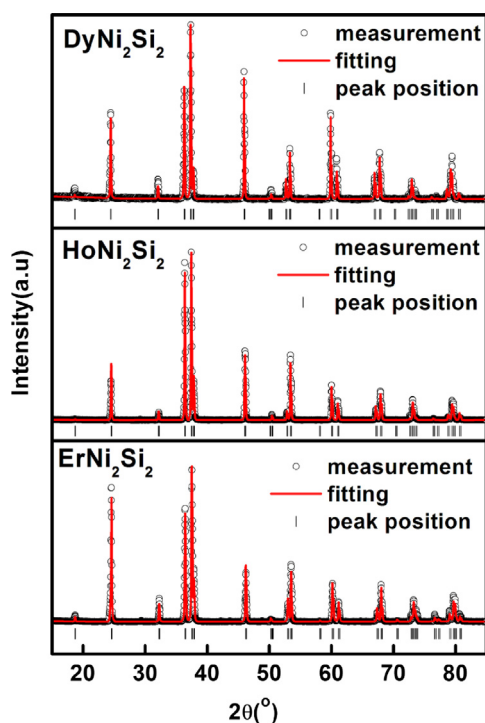


Fig. 1. Measured and refined powder X-ray diffraction (XRD) patterns of RNi_2Si_2 ($R=Dy, Ho, Er$) compounds at room temperature.

Table 1

Lattice parameters of RNi_2Si_2 ($R=Dy, Ho, Er$) compounds at room temperature.

RNi_2Si_2	a (Å)	c (Å)	a/c	v (Å ³)
$R=Dy$	3.9520	9.5425	0.414	149.039
$R=Ho$	3.9433	9.5335	0.414	148.246
$R=Er$	3.9314	9.5223	0.413	147.173

temperature. It is found that all the samples crystallize in a single phase with $ThCr_2Si_2$ -type structure (space group= $I4/mmm$). The lattice parameters were calculated by refining XRD data using the Rietveld technique. As expected, the lattice parameters and unit cell volume decrease with increasing element number of rare earth, as shown in Table 1. The almost constant value of a/c indicates these RNi_2Si_2 ($R=Dy, Ho, Er$) compounds keep a good $ThCr_2Si_2$ -type body centered tetragonal structure.

Fig. 2 shows the temperature dependences of zero-field-cooled (ZFC) and field-cooled (FC) magnetizations for RNi_2Si_2 ($R=Dy, Ho, Er$) compounds in a magnetic field of 100 Oe. For all RNi_2Si_2 ($R=Dy, Ho, Er$) compounds, no difference can be observed in the ZFC and FC curves, indicating no thermal hysteresis. Furthermore, all the samples exhibit AFM order and show sharp peaks at T_N , which are about 6.5 K for $DyNi_2Si_2$, 4.9 K for $HoNi_2Si_2$ and 3.5 K for $ErNi_2Si_2$. Compared with those in Ref. [15], each transition temperature is larger by about 0.5 K, which possible is due to the large temperature interval (1 K) in our measurement.

Fig. 3(a) and (b) shows the magnetization (M) isotherms for $DyNi_2Si_2$ compounds measured at different temperature steps in a temperature range of 2–42 K. To investigate the magnetic reversibility, the $M-H$ curves were measured in field increasing and decreasing modes. It is clearly found that the magnetization isotherms show perfectly reversible behavior with the field increasing and decreasing (see the inset of Fig. 3(a)). However, in order to clearly show the magnetization curves in this paper, we didn't show the other magnetization isotherms of RNi_2Si_2 ($R=Dy, Ho, Er$) measured in field decreasing modes. At 2 K, an obvious

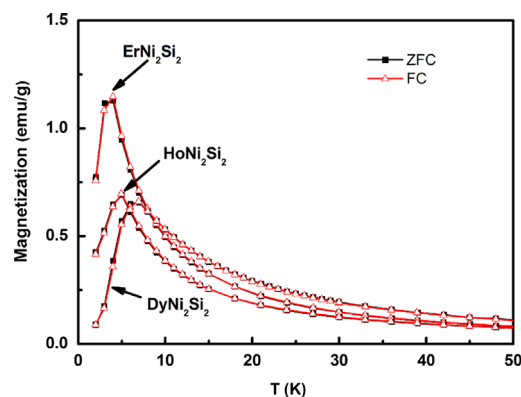


Fig. 2. Temperature dependences of zero-field-cooled (ZFC) and field-cooled (FC) magnetizations for RNi_2Si_2 ($R=Dy, Ho, Er$) compounds in a magnetic field of 100 Oe.

two-step metamagnetic transition is observed in Fig. 3(a). The multi-step metamagnetic transition phenomenon was also confirmed by other authors [16,17]. The critical field (B_c) required for metamagnetic transition is estimated. The value of B_c , defined as the maximum of $dM/dH-H$ curve, is found to be about 0.6 T and 1.5 T at 2 K for $DyNi_2Si_2$. With the temperature increasing, the metamagnetic behavior become weaker and weaker until the isothermal $M-H$ curves exhibit a FM nature at the temperature approach the T_N due to the field-induced AFM-FM transition and a PM state at the temperature much higher than T_N . Fig. 3(c) and (d) shows the Arrott plots of $DyNi_2Si_2$. According to the Banerjee criterion [18], a magnetic transition is the first-order when the slope of Arrott curves is negative, whereas it will be the second-order when the slope is positive. The S-shaped (negative slope) in the Arrott curves (see Fig. 3(c)) indicate the field-induced AFM-FM transition is first-order character. For $HoNi_2Si_2$ compound, the magnetization isotherms and the corresponding Arrott curves in the temperature range of 2–30 K are shown in Fig. 4(a)–(d). Compared with the $DyNi_2Si_2$ compound, $HoNi_2Si_2$ only exhibits a one-step metamagnetic transition with a value of $B_c=0.5$ T (see Fig. 4(a)). Furthermore, the B_c value has a small decrease with increasing temperature. The lower B_c value indicates that the $HoNi_2Si_2$ compound exhibits a weaker AFM coupling than $DyNi_2Si_2$, which is beneficial for obtaining a relatively larger MCE under low magnetic field change. With increasing temperature, the isothermal $M-H$ curves exhibit a FM nature and a PM state at the temperature close to and higher than T_N , respectively. The Arrott curves of $HoNi_2Si_2$ (see Fig. 4(a) and (d)) exhibit obviously negative slopes below T_N , confirming the existence of the field-induced first-order AFM-FM transition. Fig. 5(a)–(d) shows the magnetization isotherms and the corresponding Arrott curves for $ErNi_2Si_2$ compound in the temperature range of 2–31 K. One can find that the $ErNi_2Si_2$ compound has the smallest critical field ($B_c=0.3$ T) compared with $DyNi_2Si_2$ and $HoNi_2Si_2$. It also means that the $ErNi_2Si_2$ compound will exhibit more excellent MCE under low magnetic field change. This expectation will be demonstrated in the next part.

The values of ΔS_M for RNi_2Si_2 ($R=Dy, Ho, Er$) compounds were calculated from the magnetization versus magnetic field data using the integrated Maxwell relation $\Delta S_M(T, H) = \int_0^H (\partial M / \partial T)_H dH$. Fig. 6 shows the temperature dependences of ΔS_M for different magnetic field changes up to 7 T. As expected, the RNi_2Si_2 ($R=Dy, Ho, Er$) compounds each show large values of ΔS_M around T_N . In addition, almost the same maximal value of ΔS_M (about -25.2 Jkg⁻¹ K⁻¹) is observed for compounds with $R=Dy, Ho, Er$ under a field change of 0–7 T. For a magnetic field change of 0–5 T, the maximum values of ΔS_M are found to be -21.3 , -21.7 , and -22.9 Jkg⁻¹ K⁻¹ around T_N for RNi_2Si_2 ($R=Dy, Ho, Er$), respectively.

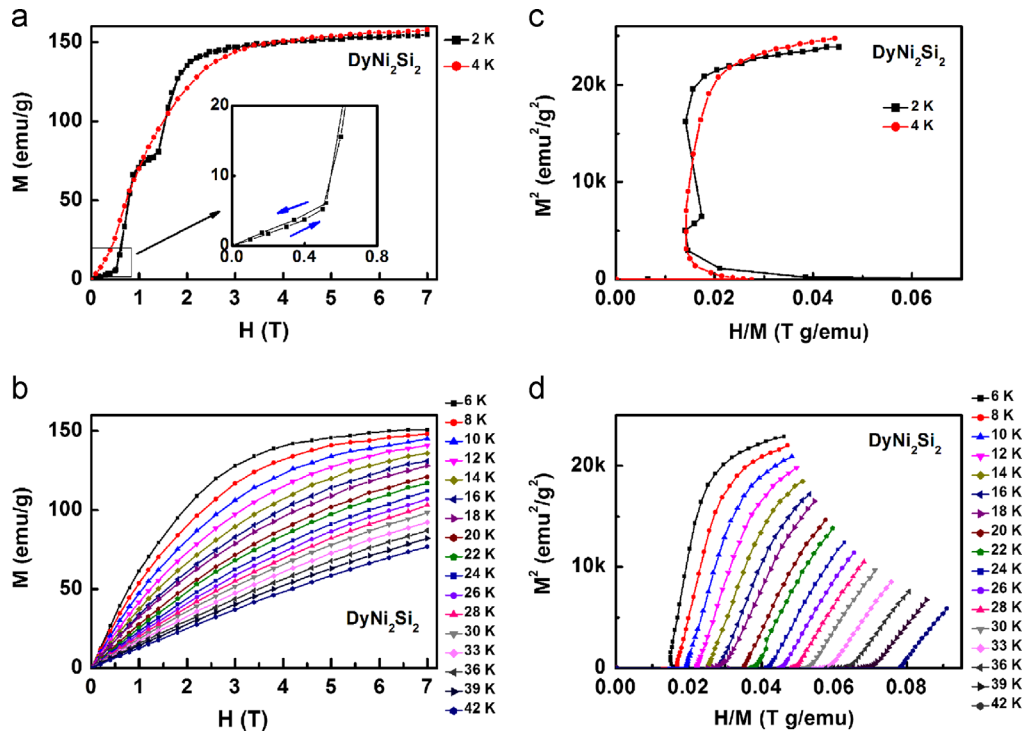


Fig. 3. (a,b) Magnetization isotherms for the DyNi_2Si_2 compound in a temperature range of 2–46 K; the inset of (a) is a highlight of the low field region. (c,d) Corresponding Arrott curves for the DyNi_2Si_2 compound.

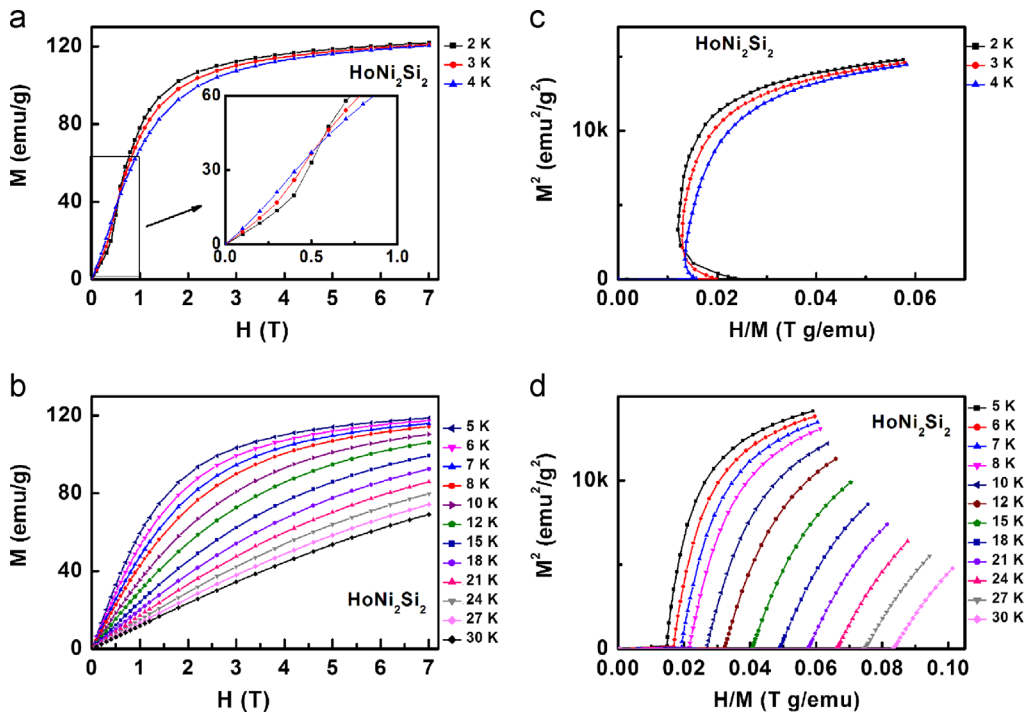


Fig. 4. (a,b) Magnetization isotherms for the HoNi_2Si_2 compound in a temperature range of 2–30 K; the inset of (a) is a highlight of the low field region. (c,d) Corresponding Arrott curves for the HoNi_2Si_2 compound.

It can be seen that the maximum values of ΔS_M are almost unchanged with the changes of rare earth element under a same field change when the applied magnetic fields are larger than 5 T. However, for a relatively low field change of 0–2 T, the maximum values of ΔS_M are -6.9 , -10.9 , and $-15.1 \text{ J kg}^{-1} \text{ K}^{-1}$ around T_N for RNi_2Si_2 ($R=\text{Dy, Ho, Er}$), respectively. The ΔS_M values under low field change rapidly increase with the increasing rare earth element number, maybe due to the decrease in the corresponding B_c .

It is noted that such giant ΔS_M values of RNi_2Si_2 ($R=\text{Dy, Ho, Er}$), especially under the low magnetic field change, are comparable to or much larger than those of the same potential magnetic-refrigerant materials in a similar magnetic transition temperature under the same field change, such as ErMn_2Si_2 [7], ErRu_2Si_2 [8], ErCr_2Si_2 [9], HoCuSi [19], Er_4NiCd [20], $\text{Dy}_{0.9}\text{Tm}_{0.1}\text{Ni}_2\text{B}_2\text{C}$ [21], ErNi_2 [22], ErNiBC [23], and $\text{HoNi}_2\text{B}_2\text{C}$ [24] (see Table 2). The low-field large MCE for RNi_2Si_2 ($R=\text{Dy, Ho, Er}$) is associated with the field-

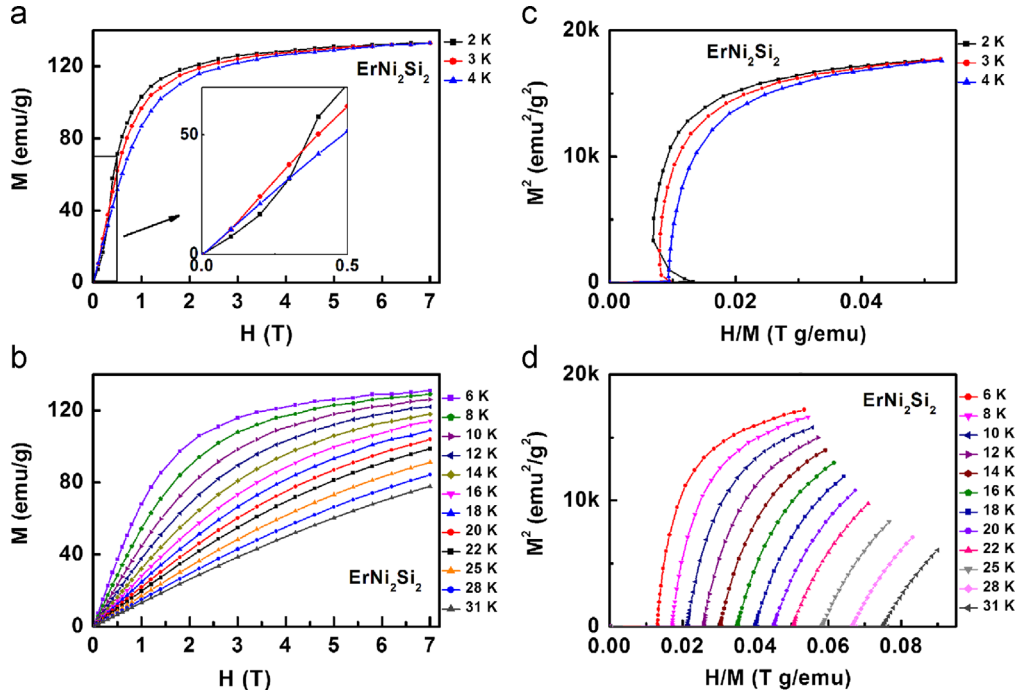


Fig. 5. (a,b) Magnetization isotherms for the ErNi_2Si_2 compound in a temperature range of 2–31 K; the inset of (a) is a highlight of the low field region. (c,d) Corresponding Arrott curves for the ErNi_2Si_2 compound.

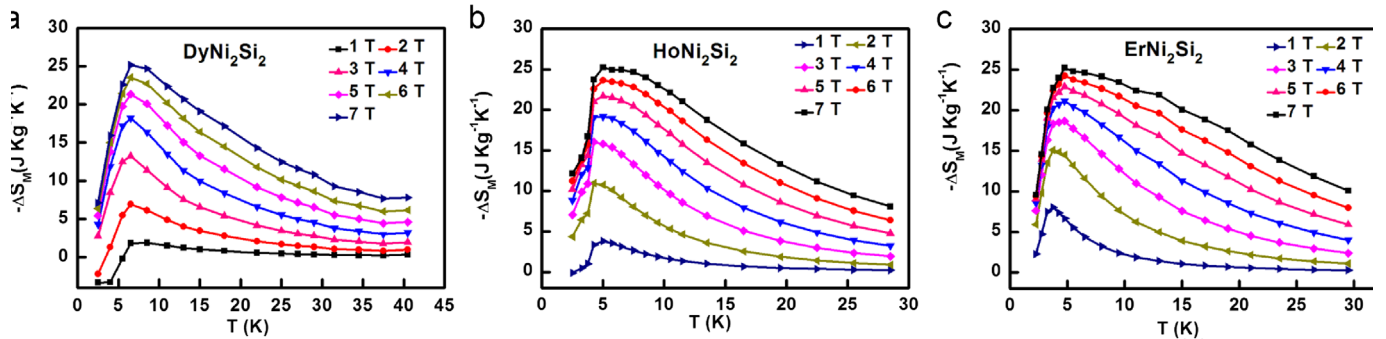


Fig. 6. Temperature dependences of isothermal magnetic entropy change ΔS_M for (a) DyNi_2Si_2 , (b) HoNi_2Si_2 , and (c) ErNi_2Si_2 compounds.

Table 2

Magnetic ordering temperature (T_0) and maximum values of ΔS_M under the field changes of 0–2 and 0–5 T for RNi_2Si_2 ($R=\text{Dy, Ho, Er}$) compounds and some potential magnetic refrigerant materials.

Material	T_0 (K)	$-\Delta S_M$ ($\text{J kg}^{-1} \text{K}^{-1}$)		Reference
		0–2 T	0–5 T	
DyNi_2Si_2	6.5	6.9	21.3	This work
HoNi_2Si_2	4.9	10.9	21.7	This work
ErNi_2Si_2	3.5	15.1	22.9	This work
ErMn_2Si_2	4.5	20	25.2	[7]
ErRu_2Si_2	5.5	11	17.6	[8]
ErCr_2Si_2	4.5	24.1	29.7	[9]
HoCuSi	7	16.7	33.1	[19]
Er_4NiCd	5.9	7.3	18.3	[20]
$\text{Dy}_{0.9}\text{TM}_{0.1}\text{Ni}_2\text{B}_2\text{C}$	9.2	4.1	14.7	[21]
ErNi_2	7	12.3	19.6	[22]
ErNiBC	5	17.1	–	[23]
$\text{HoNi}_2\text{B}_2\text{C}$	6.5	7.3	19.2	[24]

induced first-order AFM-FM metamagnetic transition and their low B_c . The large MCE under the low field changes are advantageous to the magnetic refrigeration by using the permanent magnet.

Therefore, RNi_2Si_2 ($R=\text{Dy, Ho, Er}$) compounds are probably promising candidates for practical application in low-temperature magnetic refrigeration.

4. Conclusions

The magnetic properties and MCEs for RNi_2Si_2 ($R=\text{Dy, Ho, Er}$) compounds are studied. The maximum values of ΔS_M are found to be -21.3 , -21.7 , and $-22.9 \text{ J kg}^{-1} \text{K}^{-1}$ around T_N for a magnetic field change of 0–5 T, respectively. It is notable that a large ΔS_M (such as $15.1 \text{ J kg}^{-1} \text{K}^{-1}$ at $T_N=3.5 \text{ K}$ for ErNi_2Si_2) without thermal and magnetic hysteresis losses appears under a relatively low field change of 0–2 T, which is beneficial for practical applications of magnetic refrigeration. Therefore, RNi_2Si_2 ($R=\text{Dy, Ho, Er}$) compounds probably are promising candidates for magnetic refrigeration around liquid helium temperature.

Acknowledgments

This work was supported by the National Natural Science Foundation of China, the Hi-Tech Research and Development

program of China, the Key Research Program of the Chinese Academy of Sciences, and the National Basic Research of China.

References

- [1] K.A. Gschneidner Jr, V.K. Pecharsky, *Annual Review of Materials Science* 30 (2000) 387–429.
- [2] O. Gutfleisch, M.A. Willard, E. Brück, C.H. Chen, S.G. Sankar, P. Liu, *Advanced Materials* 23 (2011) 821–842.
- [3] B.G. Shen, J.R. Sun, F.X. Hu, H.W. Zhang, *Advanced Materials* 21 (2009) 4545–4564.
- [4] N.A. de Oliveira, P.J. von Ranke, *Physics Reports* 489 (2010) 89–159.
- [5] K.A. Gschneidner Jr, V.K. Pecharsky, A.O. Tsokol, *Reports on Progress in Physics* 68 (2005) 1478–1539.
- [6] J.L. Wang, S.J. Campbell, J.M. Cadogan, A.J. Studer, R. Zeng, S.X. Dou, *Applied Physics Letters* 98 (2011) 232509.
- [7] L.W. Li, K. Nishimura, W.D. Hutchison, Z.H. Qian, D.X. Huo, T. NamiKi, *Applied Physics Letters* 100 (2012) 152403.
- [8] T. Samanta, I. Das, S. Banerjee, *Applied Physics Letters* 91 (2007) 152506.
- [9] L.W. Li, W.D. Hutchison, D.X. Huo, T. NamiKi, Z.H. Qian, K. Nishimura, *Scripta Materialia* 67 (2012) 237–240.
- [10] P. Kumar, K.G. Suresh, A.K. Nigam, A. Magnus, A.A. Coelho, S. Gama, *Physical Review B* 77 (2008) 224427.
- [11] M.S. Kim, N.H. Sung, Y. Son, M.S. Ko, B.K. Cho, *Applied Physics Letters* 98 (2011) 172509.
- [12] L.W. Li, K. Nishimura, H. Yamane, *Applied Physics Letters* 94 (2009) 102509.
- [13] L.W. Li, K. Nishimura, G. Usui, D.X. Huo, Z.H. Qian, *Intermetallics* 23 (2012) 101–105.
- [14] J.K. Yakinthos, P.F. Ikononou, *Solid State Communications* 34 (1980) 777–779.
- [15] J.M. Barandiaran, D. Gignoux, D. Schmitt, J.C. Gomezsal, J.R. Fernandez, *Journal of Magnetism and Magnetic Materials* 69 (1987) 61–70.
- [16] Y. Hadhimoto, T. Shigeoka, N. Iwata, H. Yoshizawa, Y. Oohara, M. Nishi, *Journal of Magnetism and Magnetic Materials* 140–144 (1995) 903–904.
- [17] A. Garnier, D. Gignoux, D. Schmitt, *Journal of Magnetism and Magnetic Materials* 145 (1995) 67–73.
- [18] B.K. Banerjee, *Physics Letters* 12 (1964) 16–17.
- [19] J. Chen, B.G. Shen, Q.Y. Dong, F.X. Hu, J.R. Sun, *Applied Physics Letters* 96 (2010) 152501.
- [20] W. Hermes, U.C. Rodewals, R. Pottgen, *Journal of Applied Physics* 108 (2010) 113919.
- [21] L.W. Li, K. Nishimura, *Applied Physics Letters* 95 (2009) 132505.
- [22] E.J.R. Plaza, V.S.R. de Sousa, M.S. Reis, P.J. von Ranke, *Journal of Alloys and Compounds* 505 (2010) 357–361.
- [23] L.W. Li, M. Kadonaga, D.X. Huo, Z.H. Qian, T. Namiki, K. Nishimura, *Applied Physics Letters* 101 (2012) 122401.
- [24] L.W. Li, K. Nishimura, D.X. Huo, M. Kadonaga, T. Namiki, Z.H. Qian, *Applied Physics Express* 4 (2011) 093101.